Role of Abducens Neurons in Vestibuloocular Reflex

ALEXANDER A. SKAVENSKI AND DAVID A. ROBINSON

The Clayton Laboratories, Department of Medicine, and the Department of Biomedical Engineering, The Johns Hopkins University, Baltimore, Maryland 21205

HEAD ROTATIONS produced as an animal moves in its environment lead to compensatory eye movements which prevent images from sweeping across the retina too quickly. This response is known as the vestibuloocular reflex. Its properties and neural bases have been investigated extensively (e.g., 6, 8, 12, 16, 17, 19, 20, 32, 34). Based on these studies, the simplified diagram in Fig. 1 illustrates the action of this reflex. The upper path simply illustrates that eye position in space is the mechanical difference between head position in space and eye position in the head. This path would allow head motion to disturb vision if compensatory eye movements were not generated by the brain (lower path, Fig. 1). To insure that eye position in the head is just equal and opposite to head position in space, the brain must be able to sense head position. Unfortunately, the semicircular canals are stimulated by angular acceleration of the head, the second derivative of head position. In order to recover position information to move the eye appropriately, the vestibuloocular system must perform a double integration of head acceleration; the first integration yielding a head-velocity signal and the second, a head-position signal.

The first integration is known to be accomplished mechanically within the semicircular canals themselves. Steinhausen (32) first modeled the canals after the following equation:

$$I\ddot{\phi} + \rho\dot{\phi} + K\phi = I\ddot{\theta}_h \qquad (1)$$

where ϕ is the angular displacement of the endolymph with respect to the skull; I, the moment of inertia of the endolymph; ρ, the moment of viscous drag at unit angular velocity of the endolymph with respect to the skull; K, the stiffness or cupula elastic restoring moment per unit angular deflection of the endolymph, and $\ddot{\theta}_h$, the angular acceleration of the head. Within the range of natural head movements, $I\ddot{\phi}$ and $K\phi$ are very small with respect to $\rho\dot{\phi}$, so that *equation 1* may be approximated by:

$$\rho\dot{\phi} = I\ddot{\theta}_h$$

This may be integrated directly to yield

$$\rho\phi = I\dot{\theta}_h \qquad (2)$$

From this it may be concluded that, generally, cupula displacement is not proportional to angular acceleration but to its integral, the angular velocity of the head (19). Furthermore, it has been shown that the neural discharge of primary and secondary vestibular afferents is proportional to cupula displacement, and thus to the angular velocity of the head (8, 20).

Consequently, a second integration must be performed between the primary vestibular afferents (R_v, Fig. 1) and eye position in the orbit ($\theta_{e/h}$). A portion of this integration process is known to lie in the dynamics (particularly viscous drag) of the extraocular muscles and suspensory tissues of the globe (25). The aim in the present experiments was to determine the relative contributions of brain stem neural mechanisms and orbital mechanics to this second integration. Since any head movement can be expressed as the sum of sine waves, it is convenient and sufficient, as in Fig. 1, to describe the system response to a sine wave. In that case, actions such as integration and differentiation may be described by the phase shift they introduce. Head acceleration is phase advanced from head position by 180°. The double integration of the reflex then consists of contributing a 180°

Received for publication December 4, 1972.

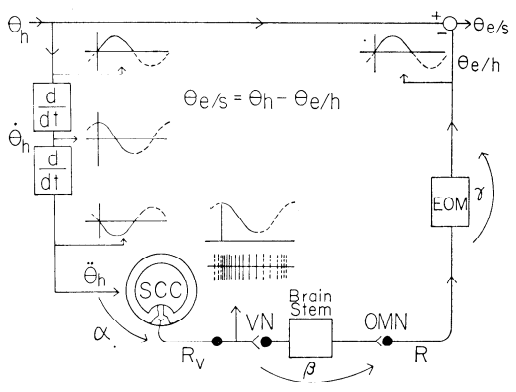

FIG. 1. Signal flow diagram illustrating the way in which the vetibuloocular reflex generates changes in eye position with respect to the head, $\theta_{e/h}$, that are opposite to changes of the head position in space, θ_h, and stabilizes eye position in space, $\theta_{e/s}$. Signals are shown for the special case of a sinusoidal head rotation so that a phase shift can be assigned to each signal-processing element. The top path shows the mechanical addition of θ_h and $\theta_{e/h}$ to produce $\theta_{e/s}$. The lower path illustrates that head acceleration, $\ddot{\theta}_h$, stimulates the semicircular canals, SCC, which integrates it ($\int dt$) with phase lag α to produce a frequency-coded signal proportional to head velocity ($\dot{\theta}_h$) in the neural dicharge pattern of the primary vestibular afferents, R_v, and in neurons in the vestibular nuclei (VN). The signal needed to drive the oculomotor neuron (OMN) discharge rate, R, is obtained by neural elements in the brain stem pathways of the vestibuloocular reflex with phase lag β. $\theta_{e/h}$ is produced by R through dynamics of the extraocular muscles, EOM, with a phase lag γ. The negative sign indicates that $\theta_{e/h}$ is opposite to θ_h and is obtained by connecting the appropriate canals and extraocular muscles. Small plots of sinusoids show the difference in form of signals as a function of time at various critical points in the model.

phase lag through the combined phase lags of α, β, and γ. Since the canals perform the first integration, α is close to a 90° lag. The sum of the brain stem lag, β, and orbital mechanics lag, γ, must add up to another 90°. Thus, one aim of the present experiments was to measure the relative contributions of β and γ to the second integration.

Actually, a preliminary prediction of γ can be made from the behavior of oculomotor neurons during visually guided eye movements (28). The prediction is that the orbital dynamics can only effectively integrate rather high-frequency signals. At lower frequencies such as 0.1 Hz, the predicted γ is very small. This makes it necessary to hypothesize that a neural integrator lies in the pathways of the vestibuloocular reflex to integrate low-frequency signals. Such a neural integrator, with its phase lag, β, is shown in Fig. 1.

The present experiments sought two critical facts necessary to confirm this prediction. First, it was necessary to show that oculomotor neurons behave in the same way for eye movements driven by natural vestibular stimulation as they do for visually guided movements. Prior studies (10, 15, 28, 31) found that all oculomotor neurons participated in the same way in each type of visually guided movement (saccades, smooth-pursuit movements, fixation, and vergence movements). It remained to be shown that these neurons also participate in the same way for the eye movements evoked by natural vestibular stimulation. The possibility of behavior differences occurs because the vestibular and visual systems are quite distinct (receptors and pathways) and could provide different inputs to the oculomotor neurons. Evidence that this possibility is not the case will be presented.

Second, it will be shown that the prediction of a neural, brain stem integrator is confirmed by direct measurements of the phase lag introduced by the orbital mechanics during sine-wave rotations of the head. In particular, during recordings made in alert, intact, and behaving monkeys, discharge patterns of motoneurons were shifted in phase from head velocity by amounts predictable only if a neural integrator lay in the path of the vestibuloocular reflex.

METHODS

Six adolescent, 6- to 7-lb. rhesus monkeys (*Macaca mulatta*) were used in this study. The procedures used have been described in detail before (15, 28) and will only be summarized briefly. Under pentobarbital sodium anesthesia and aseptic surgery, each animal was implanted with three chronic devices; namely, a crown to immobilize the head, a coil of wire around one eyeball to record eye movements, and a stereotaxically located chamber through which microelectrodes could be passed into the abducens nucleus. During recording sessions monkeys were seated in a primate chair and their heads were immobilized by clamping the crown to the chair frame. The monkeys were then placed in

two alternating magnetic fields kept in temporal and spatial quadrature which induced voltages in the eye coil permitting simultaneous recording of horizontal and vertical eye movements of one eye with a sensitivity of 0.25° arc (11). The ipsilateral abducens nucleus could be systematically explored through the stainless steel chamber with tungsten microelectrodes driven with an eccentric hydraulic drive system similar to that described by Evarts (7). Microelectrodes were coated with Insl-X and were passed through the dura and brain to the abducens nucleus within a sterile guard tube.

Prior to surgery, four of the monkeys were trained to fixate a small target display (20′ arc) to perform a foveal discrimination task for an applesauce reward. This task reduced struggling against the head restraint and helped in holding isolated motoneurons during recording sessions. It also permitted convenient calibration of the eye coil. Eye coils of the two untrained monkeys were calibrated by tranquilizing each animal and rotating its eye through known angles with a suction contact lens.

Meperidine hydrochloride (Elkins-Sinn Co.) was administered to the animals at the rate of 5 mg/kg every 4 hr for the first 2 days following surgery to minimize postoperative discomfort. The monkeys were also chronically supported with penicillin and chloramphenicol. Following a postoperative recovery period of approximately 2 weeks, daily neural recording sessions were begun on three trained monkeys. When the electrical activity of an abducens motoneuron was isolated by the microelectrode, it was recorded simultaneously with the rotations of the head and eye in the following conditions.

1) The behavior of each motoneuron during visually guided eye movements was recorded while the monkey steadily fixated the target display placed at various positions covering a range of about ± 40° arc horizontally and ± 20° arc vertically. Also, neuron behavior was recorded while the monkey made smooth-pursuit eye movements tracking objects of interest (e.g., bits of food) that were moved in its view at various velocities.

2) The behavior of each neuron was also recorded when natural vestibular nystagmus was induced by rotating the whole monkey at various constant velocities in the horizontal plane. In this condition the monkey viewed a very dimly illuminated homogeneous field (Ganzfeld) to be certain that the eyes were driven only by the vestibular system. Rotation was accomplished by mounting the eye movement-measuring system and primate chair on a pivot so that they could be rotated in the horizontal plane through an angle of about ± 165° arc. The velocity of the monkey's head (chair velocity) was continuously monitored by a tachometer generator (Inland Motor Corp., model TG-21XX-A). Chair position was monitored by integrating chair velocity on an analogue computer. In final measurements, both chair position and velocity could be resolved with a sensitivity of 0.25° arc and 0.25° arc/sec, respectively. Both were recorded along with the eye movements and neural discharges.

3) Finally, the behavior of each motoneuron was recorded when the monkey was oscillated sinusoidally at various frequencies (from 0.3 to 1.5 Hz) in the horizontal plane. The monkey again viewed a Ganzfeld. Sinusoidal chair motion was obtained by attaching the rotating chair to stationary fixtures with stiff springs to form a tuned mass-compliance system which oscillated at its natural frequency. That frequency could be altered by varying the equivalent spring stiffness.

These data provided the basis for the quantitative description of the behavior of abducens motoneurons during both visually guided eye movements and those induced by natural vestibular stimulation. The isolated cells were rather uniformly distributed over the entire volume of the abducens nucleus. Details of single-unit data analysis will be discussed with the RESULTS where appropriate.

Identification of cells as motoneurons within the abducens nucleus was done on the basis of their behavior during eye movements and on anatomy. The abducens nucleus is known to innervate the ipsilateral lateral rectus muscle exclusively and to contain few, if any, interneurons (35). In our experiments, initial identification of the abducens motoneurons was obtained by listening on an audio monitor for evidence of intense background activity correlated with ipsilateral eye movements. Later, during data reduction, care was taken to retain only those cells whose behavior corresponded to that described by previous investigators (10, 14, 15, 28, 31). Using this criterion only three cells were found whose behavior could be described as atypical. These cells were excluded from subsequent analysis because they were found to respond with a high-frequency burst of discharges following rather than preceding a saccadic eye movement and therefore, could not be described as oculomotor neurons. In addition, at the end of the neural recording sessions for each animal, several electrolytic lesions were made in known locations with respect to the recording-electrode sites. Subsequent histological examination verified that the recording sites of interest were indeed within the abducens nucleus.

These experiments were then replicated with four of the monkeys (two trained, two untrained) in which the electrical activity of multiple abducens motoneurons was recorded with a coarse microelectrode. This polyneuronal signal, very much like an EMG, was full-wave rectified and filtered by a maximally flat, second-order, low-pass filter with a bandwidth of 16 Hz. This filter smoothed the signal into a d-c voltage analogue of gross abducens nucleus activity but had a wide enough bandwidth so that its rate of change during a smooth eye movement reflected the rate of change of neural activity without distortion. This signal, like the discharge rate of a single motoneuron, was a function of both eye position and eye velocity. Thus, it produced the same type of data but represented the behavior of a pool of neurons, not just one. In this way, it enlarged the population sample on which the results were based. Again details of the quantitative treatment of this data are presented in RESULTS.

In four of the monkeys, the vestibuloocular reflex was measured for sinusoidal head rotations from 0.01 to 1.5 Hz. For the frequency range 0.01–0.07 Hz, the rotating chair was driven directly by a geared-down motor, a Scotch yoke, and a pulley system. The amplitude and phase shift of the eye movements relative to the head movements were calculated as a function of frequency.

All data were recorded on magnetic tape and retrieved on photosensitive paper by an ultraviolet mirror galvanometer recorder. Overall system bandwidth was 2 kHz.

RESULTS

Visually guided eye movements

The behavior of oculomotor neurons, in general, during fixation, smooth-pursuit movements, saccades, and vergence movements has been described in detail by other investigators (10, 14, 15, 28, 31) and will only be summarized briefly here. Oculomotor neurons fire at very constant rates when the eye is in a steady position during fixation. This discharge rate increases reasonably linearly as the eye adopts fixation positions further in the direction of action of that motoneuron's muscle (on-direction). Discharge rate is also approximately linearly related to eye velocity when the eye passes through any given constant position. Since the discharge rate of the motoneuron (R) is linearly related to both eye position (θ) and eye velocity ($d\theta/dt$), Robinson (28) suggested the following first-order approximation to relate discharge rate to eye movements:

$$R = k(\theta - \theta_T) + r\frac{d\theta}{dt} \qquad (3)$$

where k is the slope of the line relating fixation discharge rate to eye position, θ_T is the threshold or eye position at which a particular oculomotor neuron was first recruited into activity, and r is the slope of the line relating discharge rate to eye velocity at any given position. All motoneurons obey *equation 3* and differ only in the values of their characteristic parameters, k, r, and θ_T.

All the motoneurons in the present experiments behaved in this way during fixation and smooth-pursuit eye movements. Mean discharge rate was measured during fixations at a number of positions by counting the number of interspike intervals (including fractions of intervals) in a 100-msec time bin. Discharge rate was plotted as a function of eye position for each motoneuron and a straight line was fitted by eye. Thirty to sixty data points were used for each plot spread over the range of ± 40° arc. Several rate-position plots were fitted by least squares, linear regression lines. Correlation coefficients were typically 0.95. The zero intercept of this line is the threshold, θ_T; its slope is k.

During smooth eye movements the instantaneous discharge rate measurement was based on the six interspike intervals which most closely symmetrically bracketed the time at which the eye passed through a given position. Then the discharge rate due to the position of the eye (obtained from the rate-position plot) was subtracted from the instantaneous rate. The resulting change in discharge rate, due only to the velocity of the eye, was plotted for various eye velocities in the on- and off-directions and least squares, linear regression lines were fitted to these data. About 40 data points were used for each plot spread over the eye velocity range of about ± 100° arc/sec. The mean correlation coefficient was 0.91, the range was 0.72–0.97. The slope of such a rate-velocity plot is called r_{sp} in this study to distinguish it from r_{vn}, the

TABLE 1. *Slopes of lines relating discharge rate to eye position, k, and eye velocity during smooth-pursuit movements, r_{sp}, and the slow phase of vestibular nystagmus, r_{vn}, for 14 abducens motoneurons arranged in increasing values for the threshold position, θ_T, where they were first recruited into activity*

Unit	θ_T, deg arc	k, spikes/sec / deg arc	r_{sp}, spikes/sec / deg arc/sec	r_{vn}, spikes/sec / deg arc/sec
1	−44	3.3	0.30	0.58*
2	−39	3.5	0.43	0.47
3	−38	5.4	1.54	0.94*
4	−36	5.8	0.70	0.94
5	−33	4.0	0.51	0.49
6	−31	7.2	0.45	0.65
7	−30	3.6	1.56	1.41
8	−28	4.4	1.23	0.85*
9	−28	7.7	0.58	0.60
10	−24	4.5	0.53	0.47
11	−20	4.9	0.43	0.48
12	7	12.0	2.23	2.15
13	8	8.5	1.70	1.92
14	11	3.7	0.55	0.35

Negative signs signify that threshold eye position was contralateral to the primary position. *Signify those units for which r_{sp} was significantly different from r_{vn} ($P < 0.001$ in t test for significance of difference in slopes of two linear regression lines (18).

rate-velocity slope found during vestibular nystagmus.

The values k, r_{sp}, and θ_T, summarizing the behavior of 14 abducens motoneurons during visually guided eye movements, are shown in Table 1. These values are comparable to those described in previous experiments for visually guided eye movements. However, most of the cells in the present experiments were deliberately selected to have low thresholds so that they would be active even when the eye was looking in the off-direction. This selection proved useful during vestibular nystagmus and sinusoidal rotations when we had little control over the eye position about which the vestibular movements were made. In the Ganzfeld, monkeys frequently looked in the off-direction where all high-threshold motoneurons were silent. Data for a few high-threshold motoneurons have been included to show that our sampling has not biased the results.

Although many units were isolated for a sufficient time to obtain k, θ_T, and r_{sp}, it was more difficult to hold units during rotation, especially since the animals could no longer work for a food reward, became restless, and struggled. Only 14 units survived for this part of the study. Similar difficulties arose during sinusoidal rotations and only 10 units survived for the entire time required to complete all the tests.

Natural vestibular stimulation

All motoneurons also participated in the eye movements elicited by natural vestibular stimulation. To show that the units participated quantitatively in the same way as they did during visually guided eye movements, it was necessary to show that the coefficients of *equation 3* were independent of the sensory modality leading to the movements. Firing rates were selected at moments when the chair velocity passed through zero and compared to the rate-position relationship obtained with vision. No significant difference was found between the values of k and θ_T in the two cases where the animal was stationary with vision and rotating without vision. Therefore, no distinction is made in Table 1 for k and θ_T between the two cases. Values of r were obtained for the slow phase of vestibular nystagmus in exactly the same manner as outlined previously for pursuit movements and are also reproduced in Table 1 for direct comparison. Vestibular slow-phase

velocities were obtained over the range ± 100° arc/sec. The mean correlation coefficient was the same as for pursuit movements.

As can be seen in Table 1, all the cells participated in a qualitatively similar manner in both visually guided eye movements and those induced by natural vestibular stimulation, indicating that, from a functional standpoint, the oculomotor neurons serve as a single final common path and cannot be segregated according to movement type. Furthermore, 11 of the 14 units had values of r_{sp} and r_{vn} that were indistinguishable by a t test for the significance of differences in the slopes of the two linear regression lines (18). Thus, the majority of units behaved in the same way, qualitatively and quantitatively, for both types of eye movements. There are, however, slight quantitative differences in the values of r for the two kinds of movements for three cells (indicated by an asterisk in Table 1) which were statistically reliable. The implications of this will be discussed later.

Sinusoidal eye movements

The primary objective in the present experiments was to show that the orbital mechanics of the eye cannot integrate velocity signals to yield eye position over a large part of the frequency range for which the vestibuloocular reflex works adequately. This hypothesis is already suggested by *equation 3* which was just shown to be an adequate description of the motoneuron's behavior during vestibular eye movements. If the eye movement is a sine wave described by $\theta = \sin \omega t$ then it can be shown, by solving *equation 3*, that the phase lag γ between eye position and oculomotor neuron discharge rate is:

$$\gamma = \tan^{-1}(\omega \hat{T}) \qquad (4)$$

where ω is the frequency in radians per second, t is time, and $\hat{T}$ is the time constant of *equation 3* which is the ratio r/k. Values of $\hat{T}$ for 10 oculomotor neurons are reproduced in Table 2. They vary, from cell to cell, over a 4:1 range.

By substituting these time constants into *equation 4* it can be seen that the orbital mechanics only effectively integrate high frequencies; that is, only at high frequencies does γ approach 90°. For example, the mean $\hat{T}$ (159.1 msec) predicts that eye position will lag neuron discharge rate by 45° or less below a frequency of 1.0 Hz. Direct measurements during sinusoidal rotations of the monkey (Fig. 2*A*) confirmed this prediction.

TABLE 2. *Values of time constants, T, for 10 oculomotor neurons obtained from direct measurements of phase lag during natural sinusoidal rotations and those calculated, $\hat{T}$, from ratio r/k based on behavior of motoneuron during fixation and vestibular nystagmus**

Unit	T, msec	$\hat{T}$, msec
2	165	133
4	347	162
5	236	122
6	133	91
7	274	392
8	176	193
9	140	78
11	121	99
13	220	226
14	234	95
Mean ± SD	204.6 ± 71.4	159.1 ± 94.8

* These cells are a subset of Table 1 and retain the same identity number used there.

For each of the 10 cells for which isolation was maintained through the sinusoidal oscillations, the phase relation between motoneuron discharge rate and eye position with respect to the head was measured at frequencies ranging from 0.3 to 1.5 Hz. Parts of the records were selected where the compensatory eye movement was uninterrupted by a quick phase over a sufficient portion of the sine wave to estimate the location of a minimum or a maximum in both eye position and neural discharge rate. Generally, such records included more than one complete cycle at higher frequencies. However, at lower frequencies this was rarely possible and measurements were made for only a half-cycle (about 180°) containing either a maximum or minimum. The instantaneous discharge rate was then calculated (reciprocal of interspike interval) for each half-cycle and the minima or maxima were obtained as the point midway between instants where the discharge rate was the same. The phase shift, γ, between

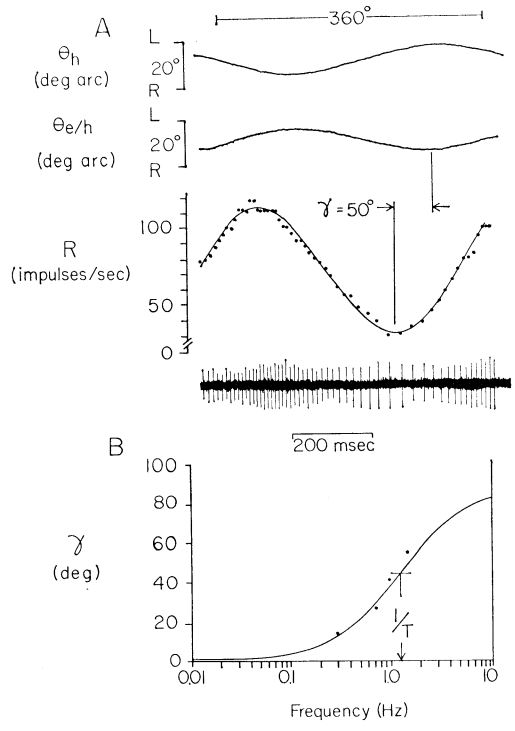

FIG. 2. *A*: illustration of the phase lag, γ, between eye position in the head, $\theta_{e/h}$, and the firing of an abducens motoneuron (bottom trace) during sinusoidal rotation of the head in space, θ_h. Neural discharge rate, R, was smoothed over two interspike intervals. *B:* data points (●) show mean phase lags (N ≧ 4) between eye position and abducens discharge rate at four different frequencies for a typical unit (no. 9, Table 1). Phase lag is plotted upward. Details of the curve fitted to these data points (solid line) are described in the text.

firing-rate maxima or minima and eye-position maxima or minima was then measured as illustrated in Fig. 2*A*.

Mean phase shifts, based on at least two maxima and two minima at each frequency, summarizing the behavior of one typical motoneuron (unit 9, Tables 1 and 2) during sinusoidal oscillations are plotted as a function of frequency in the Bode diagram of Fig. 2*B*. The predicted curve from *equation 4* is also shown in Fig. 2*B* where a value for the time constant, $\hat{T}$, was chosen to give the best fit by eye (varying $\hat{T}$ in *equation 4* simply slides the curve in Fig. 2*B* to the left or right). Figure 2*B* shows that *equation 4* correctly predicts the behavior of phase shift as a function of frequency. After the curve was fitted to the data, the measured time constant, T, was obtained by noting that frequency, f, for which the curve has the value 45°. Then, $T = 1/(2\pi f)$. Values of T, from phase shift data, for 10 oculomotor neurons are shown in Table 2 along with the estimated values of the time constant, $\hat{T}$, obtained by calculating the ratio r/k for the same motoneurons using the value r_{vn}.

There were large quantitative differences between the estimated values, $\hat{T}$, and the measured time constants, T (sometimes greater than 2:1). However, there is one point about which both agree; namely, over a large-frequency range (all frequencies less than about 1 Hz) the phase lag introduced by the mechanics of the orbital contents is small (less than 45°). For example, at 0.1 Hz the mean measured time constant, T, indicates (from *equation 4*) that γ is only 7.5° and the mean estimated time constant, $\hat{T}$, indicates that γ is only 6°. Thus, a large phase lag (about 83° at 0.1 Hz) must be inserted in the pathways of the vestibulo-ocular reflex by a central neural mechanism (β, Fig. 1).

Behavior of small groups of motoneurons during vestibular nystagmus

The behavior of small groups of abducens motoneurons (we estimate four or more) is similar to that of single motoneurons. A total of 10 recording sites were analyzed in four monkeys (one site in each of two trained monkeys and four sites in each of the two untrained monkeys). In general, the methods of data analysis were identical to those described for the isolated motoneurons with the exception that we measured the average (mean) d-c voltage of the amplified and rectified gross potential during fixation and the change in the average d-c voltage during pursuit eye movements and the slow phases of vestibular nystagmus. This resulted in an equation similar to *equation 3* in which k and r have the dimensions microvolts per degree arc and microvolts per degree arc per second. The absolute values of these numbers are unimportant but their ratio, the time constant, is.

All 10 recording sites participated in

fixation, smooth-pursuit movements, and vestibular nystagmus. The mean estimated time constant (r/k) for the gross potentials was 137.8 msec (standard deviation = 30.4 msec). The means of the time constants estimated by smooth-pursuit movements and vestibular nystagmus differed by only 7 msec. At six sites, the two time constants differed by less than 24 msec. For these time constants, r_{sp} and r_{vn} were not significantly different. At four sites the time constants differed by 36, 51, 58, and 79 msec. These differences were due to statistically reliable differences ($P \leqslant 0.01$, $N = 70$) in the values of r_{vn} and r_{sp} going into the calculation of $\hat{T}$. For a given eye velocity, then, these neuron groups were more active for one type of eye movement than another but there were no consistent trends. The mean time constant agrees roughly with those found for single units (Table 2) and reinforces the conclusion that over a broad-frequency range a neural network must insert a large phase lag in the pathways of the vestibuloocular reflex.

Eye movements during sinusoidal rotations

Our argument that a neural, phase-lagging network (i.e., an integrator) must lie in the pathways of the vestibuloocular reflex depends on the knowledge that, over the frequency range studied, the eye movements are truly compensatory for sinusoidal changes in head position. Evidence that this was indeed the case was obtained by measuring the gain and phase of eye position in the head with respect to body position in space over the frequency range 0.01–1.5 Hz. These measurements were made in four intact monkeys prior to the time any electrode penetrations were made in their brains and while the monkeys viewed a dim Ganzfeld or, in some cases, were in complete darkness. All the monkeys had spontaneous nystagmus in the dark or a dim Ganzfeld. The eye velocities (up to 5° arc/sec) and directions of the slow phases were idiosyncratic and did not vary with time or eye position. At all frequencies this spontaneous velocity was subtracted out first. Then, gain was taken as the peak change in horizontal eye velocity divided by peak change in head velocity. Phase was determined as the difference between velocity maxima or minima for head and eye movements.

The results indicate that the vestibular system generates compensatory eye movements over a surprisingly large frequency range. Gains were approximately constant over the range 0.02–1.5 Hz and had mean values of about 0.86 and 0.83 in the two trained monkeys and 1.08 and 1.51 in the two untrained monkeys. The large gain values for the two untrained monkeys reflect the fact that their eye coils could only be calibrated by rotating their eyes through known angles with a suction contact lens which probably slipped. For our purposes, it was only important to know that the gain was constant over the frequency range studied. The true value of gain is probably about 0.85 as in the two trained animals. All four animals showed a slight rise in gain (about 1.7 dB) at 0.01 Hz.

The mean phase relation between eye and head position is shown by the bottom curve ($\theta_{e/h}$) of the Bode plot in Fig. 3. Over the frequency range 0.04–1.5 Hz the eye was approximately in phase with head position (with a slight, but persistent 3° lead). At lower frequencies the phase lead was quite small; only 6.5° at 0.03 Hz and 20° at 0.01 Hz.

DISCUSSION

The results indicate, first, that oculomotor neurons participate in a similar way in the eye movements driven by vestibular stimulation and those guided by the visual system. Thus, in general, the neurons in the oculomotor nuclei are indifferent to the source of the signal that is driving the eye movements. Each neuron participated in all types of eye movements and their discharge rates were related only to the position and velocity of the eye. This finding further supports the argument that the final common path cannot be divided into separate parts, each serving a particular type of eye movement or into tonic and phasic motor systems (15). This implies that differences in extraocular muscle fiber type (e.g., see ref 23) cannot be simply cor-

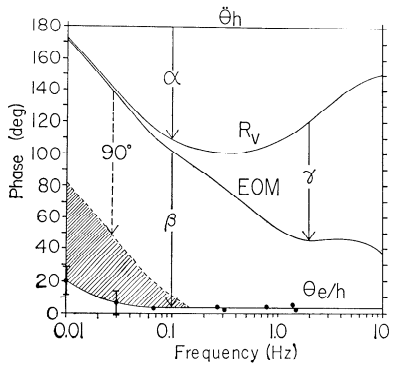

FIG. 3. Bode diagram summarizing the phase shifts with respect to head position, of discharges of primary afferents from the semicircular canals, R_v, dynamics of extraocular muscles and orbital mechanics, EOM, and eye position, $\theta_{e/h}$, for various frequencies of sinusoidal head rotation. Moving upward in this graph shows a phase lead and downward a phase lag. The top horizontal line, $\ddot{\theta}_h$, is head acceleration which leads the head position (the bottom line) by 180°. From the top line, the phase lag α of the semicircular canals (8) is subtracted to obtain the curve R_v. From that curve, the phase lag γ of the orbital mechanics (from *equation 4*) is again subtracted to produce curve EOM. The difference, β, between curves EOM and $\theta_{e/h}$ is the phase that must be contributed by a brain stem neural mechanism. Each mean phase shift in $\theta_{e/h}$ at 0.01 and 0.03 Hz was based on about 30 measurements; vertical bars show one standard deviation on each side of the mean. At higher frequencies, fewer measures of phase were needed ($N \geq 4$) and the variability (not shown) was less. The lined area at the left indicates the region in which the phase lag introduced by the neural integrator, β, must exceed 90°.

related with eye-movement type. The various extraocular muscle fiber types are much more likely to be related to fatigability (2, 15).

Moreover, the majority of units or groups of units behaved quantitatively, as well as qualitatively, in the same way for visual and vestibular inputs; i.e., they obeyed *equation 3* and had the same values of k, r, and θ_T for both types of eye movements. However, for 3 of the 14 isolated motoneurons and 4 of the 10 polyunit recording sites, the constant relating neuron activity to eye velocity during pursuit movements (r_{sp}) was reliably different from that obtained during vestibular nystagmus (r_{vn}). This might be expected since the signals driving eye velocity arrive at the motoneuron from separate neural pathways. To illustrate, assume that fibers carrying velocity information from either the visual or vestibular systems ramify in the nucleus and synaptically couple to different oculomotor neurons with a small degree of variability. Then individual neurons could be driven differently by the two velocity signals, even though the same average motoneuron pool activity created the same eye velocity; namely, they would display the modality variations observed in the present experiments. This could occur even if the two signals were mixed at a premotor level so that they shared one or more common premotor neurons. However, intuitively, it seems less likely that such differences would be observed as the number of shared neurons (and so mixing) increases. The tentative conclusion from this is that position commands, either visual or vestibular, may come from a common prenuclear source but velocity commands probably arrive directly at the motoneurons from their different sources with little or no mixing.

One should not overlook the fact that all these differences were somewhat subtle. In no case was a motoneuron observed that was exclusively driven by only one of these systems. The small differences seen probably average out to zero over the population. It may be concluded then, that on the whole, the oculomotor neurons behave in the same way for eye movements driven by either the vestibular or visual systems.

The second finding of the present experiments is that there must be a neural network in the pathways of the vestibulooocular reflex that converts velocity information from the semicircular canals into position information. That this neural integrator must exist may be seen in the Bode diagram in Fig. 3 where the known phase behavior of the semicircular canals, extraocular muscle mechanics, and the entire reflex have been summarized as a function of frequency for sinusoidal head rotations.

The upper curve (R_v) shows the phase lag, α, between head angular acceleration ($\ddot{\theta}_h$) and neural discharges in the primary vestibular afferents described by Fernandez and Goldberg's (8) mean transfer function for the spider monkey. The middle curve (EOM) shows the phase lag, α plus γ, due to the combination of canals and dynamics

of the orbital mechanics. The latter, γ, was obtained by using the mean time constant of 204.6 msec from Table 2 in *equation 4*. Since our data were only obtained up to 1.5 Hz, the curve for γ has been extrapolated according to *equation 4* with the addition of the phase lag due to a known 8-msec pure delay due mostly to excitation-contraction coupling (28). It must be recognized, of course, that at these high frequencies γ is still an underestimate of the probable phase lag due to orbital mechanics because the latter is at least a fourth-order system (27). The curve for γ shown here is correct, however, below 1.5 Hz. The bottommost curve, $\theta_{e/h}$, shows the phase relation between eye position and head position already described. This curve, too, has been extrapolated as constant above 1.5 Hz to at least 5 Hz on the basis of Benson's (1) measurements on human subjects.

Most important, these curves show that the combination of phase lags due to the canals and the orbital mechanics is not sufficient to account for the measured phase relation between eye and head position over a wide frequency range. For example, the arrow at 0.1 Hz shows that an additional 98° phase lag (β) must be introduced by the brain stem. Therefore, we must conclude that over a wide frequency range around 0.1 Hz there must be a neural network that integrates head velocity signals to produce head position information and introduce a large phase lag (about 90°) in the pathway(s) of the vestibuloocular reflex; a finding that supports Robinson's (26, 29) and Collewijn's (5) earlier speculation and which has been independently suggested by Carpenter (3).

The location of this integrator is an important question. From the works of Lorente de Nó (16) and Szentágothai (34) it is generally believed to lie in the pontine reticular formation outside of the medial longitudinal fasciculus (mlf). Here, delayed polysynaptic potentials are conveyed from the vestibular to the oculomotor nuclei and systems of reverberating collaterals are seen. Rosen (30) has offered one way of constructing a neural integrator using such a system of reverberating collaterals. The best confirmation of this view comes from Cohen and Komatsuzaki (4) who obtained ramp eye movements on stimulating the paramedian pontine reticular formation. Alternatively, Carpenter (3) has offered proof that the integrator lies in the cerebellum. It should be remarked that one hypothesis is that the integrator is formed by a velocity feedback circuit from extraocular muscle proprioception. Since there is no stretch reflex in the rhesus monkey (14) but stretch afferents are reported in the cerebellar vermis (9), the feedback loop may be closed through the cerebellum. This possibility, if taken at face value, seems unlikely because Carpenter (3) has demonstrated that opening the feedback loop from the proprioceptors of one eye does not effect the vestibuloocular reflex as measured by EMG. However, we must still leave open the possibility that proprioceptive feedback plays a role in the integration process because this process may be much more complicated than is currently suspected.

An unusual feature of the curve $\theta_{e/h}$ in Fig. 3 is the very small phase lead at low frequencies. If one used the 20° phase lead at 0.01 Hz to calculate the predicted long time constant of the semicircular canals, it would be 43 sec. This is surprisingly large compared to the value of 10 sec commonly given for man (e.g., ref 13, 19, 36), or 5.7 sec for the squirrel monkey (8), or 4 sec for the cat (21). This result was so unusual that great care was taken to insure that the animals had no visual cues. Also, for one monkey, auditory white noise was used to preclude the possibility of sound localization assisting the reflex. In preliminary experiments on cats we have found that they also have small phase leads at 0.01 Hz; too small to be commensurate with what one would predict from their semicircular canal time constants. If this is correct, it means that in cat and monkey, the slow-phase eye velocity and the behavior of vestibular neurons give quite different estimates of cupula behavior. It seems more likely that the latter would give a truer estimate of the cupula time constant than the former. Since the value of 10 sec commonly used for man is based largely on eye velocity calculations it could, by analogy with cat and monkey, be quite incorrect.

It would appear that the brain is somehow using vestibular signals to compensate the inadequate performance of the canals and extend the low-frequency working range of the vestibuloocular reflex. Specifically, at 0.01 Hz, the phase lag of canals and extraocular muscle together is only 10° and the observed eye/head phase lead is 20°. Therefore, the angle β must be 150° to make up a total of 180°. A perfect neural integrator has a phase lag of only 90° so that it is necessary to hypothesize yet another neural integrator to explain the observed phase shifts. The lined area in Fig. 3 shows the frequency region where β exceeds 90° and the amount by which it does so. This is the region where a single integrator is inadequate and some sort of low-frequency compensation for the canals themselves is needed.

The phase shift at low frequencies is complicated by another factor. Sugie and Melvill Jones (33) have pointed out that each quick phase might influence subsequent slow-phase velocity and therefore might introduce a phase lag during sinusoidal stimulation. That would predict a different phase shift with and without quick phases. Put another way, if the neural integrator is leaky, but is repeatedly reset by quick phases, its time constant need only be large enough to integrate well from one quick phase to the next. In this way a very leaky integrator could appear to have a time constant much longer than it actually had and even produce a phase shift greater than 90°. This theory has been further developed by Outerbridge (22). These authors have suggested that the leaky neural integrator has a time constant of only 1 sec. Such a short time constant predicts a phase lead in $\theta_{e/h}$ of 28° at 0.3 Hz when quick phases are absent. As shown in Fig. 3, the lead was only 3° and did not depend on whether or not quick phases were present. Thus, the time constant of the neural integrator is certainly much larger than 1 sec. However, whenever the frequency of oscillation is near, or less than, $1/2\ \pi$ times the reciprocal of the integrator time constant, the phase lag introduced by the Sugie-Melvill Jones quick-phase effect could become quite significant and may explain some of the phase lag that lies in the lined region of Fig. 3.

At the high-frequency end of Fig. 3, the opposite problem occurs; above 0.15 Hz, less than a 90° phase lag is required for β. At 2 Hz only a 45° lag is required. Since γ is undoubtedly underestimated above 2 Hz (see previous discussion of Fig. 3) the required shift β is probably less than that shown and near zero around 8–10 Hz. This means that the neural integrator must be situated in such a way that its phase lag of 90° forms less and less of a contribution at higher frequencies. Fortunately, this requirement fits in very well with the presence of the mlf. A part of the mlf is a monosynaptic relay from secondary vestibular to oculomotor neurons and might be much too simple a structure to perform integration by itself. This part therefore lies in parallel with the integrator as shown in Fig. 4 and could pass raw velocity information to the motoneurons.

To illustrate the result of this parallel combination, let the gain of this mlf transmission be T. The Laplace transform of the neural integrator is (1/s) where s is the

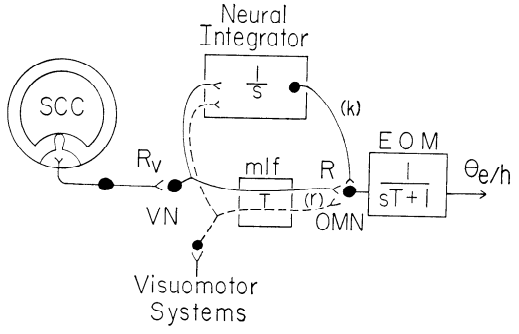

FIG. 4. A simplified model of the vestibuloocular reflex showing the role of the direct relay part of the medial longitudinal fasciculus (mlf) in the information transmission pathways between the semicircular canals and the oculomotor neurons. Symbols are the same as in Fig. 1. We suggest that the direct pathway of the mlf, which provides velocity feed forward with a gain T, is in parallel with a neural network located in the brain stem which integrates head velocity information to provide the OMN with position information. The transfer functions of the integrator and EOM are shown in Laplace transform notation. The suggestion that these vestibular paths are shared by visually driven oculomotor systems is also shown.

complex frequency variable. The transfer function of the combined pathways in Fig. 4 is,

$$\frac{R}{R_v}(s) = T + \frac{1}{s} = \frac{sT + 1}{s} \qquad (5)$$

The numerator on the right side is called a lead element because it introduces a phase lead at higher frequencies. This reduces the net phase lag just as required for β by the curves in Fig. 3.

The purpose of this phase lead departure from plain integration is to compensate the phase lag created by the orbital mechanics described by *equation 3* and shown in Fig. 2*B*. If that equation is combined with a similar one for the antagonist muscle, so that the θ_T term drops out, then, except for an arbitrary gain constant (1/k) the transfer function of the orbital mechanics is,

$$\frac{\theta_{e/h}}{R}(s) = \frac{1}{sT + 1} \qquad (6)$$

where T is the ratio r/k.

The total transfer function of eye position from vestibular neuron discharge rate is then,

$$\frac{\theta_{e/h}}{R_v}(s) = \frac{(sT + 1)}{s} \times \frac{1}{(sT + 1)} = \frac{1}{s} \qquad (7)$$

that is, the lead element formed by the direct part of the mlf cancels the lag of the orbital contents so that eye position continues to be the integral (*equation 7*) of vestibular neuron activity at high frequencies.

In other words, high-frequency oscillations (roughly, above 1 Hz) are shunted by the mlf and integrated by the orbital mechanics, while low frequencies (below 1 Hz) are integrated by the neural integrator. This velocity feed-forward path probably explains why the vestibuloocular reflex works well up to at least 5 Hz (1). Without this path, the mechanics of the orbital tissues would cause the eye to lag very far out of phase behind changes in head position at this frequency. It may also be noted that Fernandez and Goldberg (8) found that the primary vestibular afferents do not report cupula position alone, but also are stimulated by its rate of displacement. This causes the curve for α in Fig. 3 to change from a relative phase lag at low frequencies to a relative phase lead at high frequencies. This constitutes yet another lead element with a time constant of 50 msec (8). Since the orbital mechanics contain multiple lag elements (27) we suggest that multiple lead elements are very necessary for correct performance at high frequencies. The vestibular receptor itself, just mentioned, provides one such lead element in the region of 3.2 Hz and we propose that the direct relay part of the mlf provides another lead element in the region of 0.8 Hz.

The scheme in Fig. 4 also explains another phenomenon seen in Tables 1 and 2. Two neurons (such as numbers 2 and 7) can have almost the same value of k (3.5 and 3.6) and yet have different values of r (0.43 and 1.56, respectively, for r_{sp}). These two units also have similar thresholds, yet unit 2 has a time constant (r_{sp}/k) of 123 msec, while unit 7 has a time constant of 433 msec; a ratio of 3.5:1. This suggests that position commands (which determine k) and velocity commands (which determine r) arrive at the motoneurons on two sets of fibers from different sources. If they arrived on the same set, all neurons should have the same ratio r/k unless the premotor neurons themselves were driven differentially by position and velocity commands and there was very little mixing in the motor nucleus; i.e., each neuron received synapses from only one or two incoming fibers so that differences would not average out. In any case, it seems necessary to hypothesize two separate pathways, one mediating eye-position information, the other eye-velocity information. Such an arrangement occurs automatically with the scheme in Fig. 4; the mlf carries a velocity signal, the integrator produces a position signal.

Finally, one cannot avoid wondering whether or not the neural integrator for the vestibular system might not also be shared with the visually guided eye-movement systems as illustrated in Fig. 4. Recent models of these systems have in common at least one neural integrator in the pathways to the oculomotor neurons (e.g., see Collewijn (5) for the optokinetic system,

Rashbass and Westheimer (24) for the vergence system, and Young and Stark (37) for the saccadic system). Although these models lack neurophysiological supporting evidence, they do account for a variety of open- and closed-loop visual tracking behaviors. It is tempting to think that the final integrator proposed separately by each of these models might actually be only one shared integrator; the same one used by the vestibular system. Weak evidence for this suggestion comes from the observation that the value of k for a given oculomotor neuron has never been observed to depend on the mode by which the eye was driven to any position. If there were separate integrators with slight variability in their coupling to individual motoneurons, we would expect, at least occasionally, to see differences in the value of k depending on eye movement type. In the present experiments we specifically searched for evidence for this but failed to find it. This is at least compatible with the idea that the integrator for the vestibular system is shared with the visual system.

SUMMARY

1. Abducens motoneuron discharge rate was recorded in alert, intact rhesus monkeys during fixation, smooth-pursuit movements, vestibular nystagmus, and sinusoidal head and body rotations.

2. The relationship between discharge rate and eye position did not change when eye position was determined by visual or vestibular stimulation.

3. In general, no difference was found in the relationship between discharge rate modulation and eye velocity when eye velocity was induced by visual or vestibular stimulation.

4. However, at a few sites, motoneurons and groups of motoneurons fired slightly differently during eye velocity driven by visual or vestibular stimulation. This difference simply indicated probable local variations in synaptic density of the fibers relaying discharges from the two origins of eye-velocity commands to the oculomotor neurons.

5. The above results, combined with previous reports, indicate that motoneuron behavior is determined only by eye position and velocity and is not determined by the type (saccade, pursuit, vergence, or vestibular) of eye movement that created the position or velocity.

6. Changes of eye position in the head were equal and opposite to changes of head position in space over the range of about 0.01–1.5 Hz during sinusoidal rotations without vision.

7. During sinusoidal rotations in the dark, the phase shift between motoneuron firing rate and eye position agreed with that predicted from the equation relating discharge rate to eye position and velocity; specifically, the phase shift of the orbital mechanics decreased rapidly from about 45° at 1 Hz to less than 7° at 0.1 Hz.

8. Since the semicircular canals are stimulated by head acceleration, the second derivative of head position, the main function of the vestibuloocular reflex is to recover the original head-position signal by doubly integrating head acceleration. The semicircular canals perform the first integration mechanically. The discharge rate of vestibular neurons is proportional to head velocity. Since the orbital mechanics have been demonstrated to be incapable of performing the second integration (which requires a 90° phase lag), it is certain that there exists a neural integrator in the brain stem between the vestibular and oculomotor nuclei which converts eye-velocity signals to eye-position signals.

ACKNOWLEDGMENTS

The authors thank R. W. Bittrick and A. R. Friendlich for their valuable technical assistance and Andrea McCracken for typing the manuscript.

Most of the information contained in this paper was reported at the Society for Neuroscience Meeting of November 1971 in Washington, D.C.

This research was supported by Public Health Service Training Grant 5 T01 GM00576 from the Institute of General Medical Sciences and by Research Grants 5 Rol EY00598 and 1 R01 EY01049 from the National Eye Institute.

Present address of A. A. Skavenski: Northeastern University. Dept. of Psychology, 440 United Realty Building, Boston, Mass. 02115.

Present address of D. A. Robinson: The Johns Hopkins University, Dept. of Ophthalmology, Woods Research Building of the Wilmer Institute, Baltimore, Md. 21205.

REFERENCES

1. BENSON, A. J. Interactions between semicircular canals and gravireceptors. In: *Recent Advances in Aerospace Medicine*, edited by D. E. Busby. Dordrecht: Reidel, 1970, p. 249–261.
2. BURKE, R. E., LEVINE, D. N., AND ZAJAC, F. E. III. Mammalian motor units: physiological-histochemical correlations in three types in cat gastrocnemius. *Science* 174: 709–712, 1971.
3. CARPENTER, R. H. S. Cerebellectomy and the transfer function of the vestibuloocular reflex in the decerebrate cat. *Proc. Roy. Soc. London, Ser. B* 181: 353–374, 1972.
4. COHEN, B AND KOMATSUZAKI, A. Eye movements induced by stimulation of the pontine reticular formation: evidence for integration in oculomotor pathways. *Exptl. Neurol.* 36: 101–117, 1972.
5. COLLEWIJN, H. An analog model of the rabbit's optokinetic system. *Brain Res.* 36: 71–88, 1972.
6. EGMOND, A. J. VAN, GROEN, J. J., AND JONGKEES, L. B. W. The mechanics of the semicircular canal. *J. Physiol., London* 110: 1–17, 1949.
7. EVARTS, E. V. A technique for recording activity of subcortical neurons in moving animals. *Electroencephalog. Clin. Neurophysiol.* 24: 83–86, 1968.
8. FERNANDEZ, C. AND GOLDBERG, J. M. Physiology of peripheral neurons innervating semicircular canals of the squirrel monkey. II. Response to sinusoidal stimulation and dynamics of peripheral vestibular system. *J. Neurophysiol.* 34: 661–675, 1971.
9. FUCHS, A. F. AND KORNHUBER, H. H. Extraocular muscle afferents to the cerebellum of the cat. *J. Physiol., London* 200: 713–722, 1969.
10. FUCHS, A. F. AND LUSCHEI, E. S. Firing patterns of abducens neurons of alert monkeys in relationship to horizontal eye movement. *J. Neurophysiol.* 33: 382–392, 1970.
11. FUCHS, A. F. AND ROBINSON, D. A. A method for measuring horizontal and vertical eye movement chronically in the monkey. *J. Appl. Physiol.* 21: 1068–1070, 1966.
12. GROEN, J. J., LOWENSTEIN, O., AND VENDRIK, A. J. H. The mechanical analysis of the responses from the end-organs of the horizontal semicircular canal in the isolated elasmobranch labyrinth. *J. Physiol., London* 117: 329–346, 1952.
13. HIXON, W. C. AND NIVEN, J. I. *Application of the System Transfer Function Concept to a Mathematical Description of the Labyrinth. I. Steady State Nystagmus Response to Semicircular Canal Stimulation by Angular Acceleration.* Bu. Med. and Surg. Proj. MR 005.13–6001, Subtask 1, Rept. no. 57, NASA Ord. no. R–1.
14. KELLER, E. L. AND ROBINSON, D. A. Absence of a stretch reflex in extraocular muscles of the monkey. *J. Neurophysiol.* 34: 908–919, 1971.
15. KELLER, E. L. AND ROBINSON, D. A. Abducens unit behavior in the monkey during vergence movements. *Vision Res.* 12: 369–382, 1972.
16. LORENTE DE NÓ, R. Vestibuloocular reflex arc. *Arch. Neurol. Psychiat.* 30: 245–291, 1933.
17. LOWENSTEIN, O. AND SAND, A. The mechanism of the semicircular canal. A study of the responses of single fiber preparations to angular accelerations and to rotation at constant speed. *Proc. Roy. Soc. Biol.* 129: 256–275, 1940.
18. MCNEMAR, Q. *Psychological Statistics.* New York: Wiley, 1962.
19. MELVILL JONES, G. AND MILSUM, J. H. Spatial and dynamic aspects of visual fixation. *IEEE Trans. Bio-Med. Eng.* 12: 54–62, 1965.
20. MELVILL JONES, G. AND MILSUM, J. H. Characteristics of neural transmission from the semicircular canal to the vestibular nuclei of cats. *J. Physiol., London* 209: 295–316, 1970.
21. MELVILL JONES, G. AND MILSUM, J. H. Frequency-response analysis of central vestibular unit activity resulting from rotational stimulation of the semicircular canals. *J. Physiol., London* 219: 191–215, 1971.
22. OUTERBRIDGE, J. *Experimental and Theoretical Study of Reflex Vestibular Control of Head and Eye Movement* (Ph.D. Dissertation). Montreal: McGill University, 1969.
23. PEACHEY, L. D. The structure of the extraocular muscle fibers of mammals. In: *The Control of Eye Movements,* edited by P. Bach-y-Rita and C. C. Collins. New York: Academic, 1971, p. 47–66.
24. RASHBASS, C. AND WESTHEIMER, G. Disjunctive eye movements. *J. Physiol., London* 159: 339–360, 1961.
25. ROBINSON, D. A. The mechanics of human saccadic eye movement. *J. Physiol., London* 174: 245–264, 1964.
26. ROBINSON, D. A. Eye movement control in primates. *Science* 161: 1219–1224, 1968.
27. ROBINSON, D. A. The oculomotor control system: a review. *Proc. IEEE* 56: 1032–1049, 1968.
28. ROBINSON, D. A. Oculomotor unit behavior in the monkey. *J. Neurophysiol.* 33: 393–404, 1970.
29. ROBINSON, D. A. Models of oculomotor neural organization. In: The *Control of Eye Movements,* edited by P. Bach-y-Rita and C. C. Collins. New York: Academic, 1971, p. 519–538.
30. ROSEN, M. J. A theoretical neural integrator. *IEEE Trans. Bio-Med. Eng.* 19: 362–367, 1972.
31. SCHILLER, P. H. The discharge characteristics of single units in the oculomotor and abducens nuclei of the unanesthetized monkey. *Exptl. Brain Res.* 10: 347–362, 1970.
32. STEINHAUSEN, W. Über die beobachtung der cupula in den Bogengangsampullen des Labyrinths des Lebenden Hechts. *Arch. Ges. Physiol.* 232: 500–512, 1933.
33. SUGIE, N. AND MELVILLE JONES, G. A model of eye movements induced by head rotation. *IEEE Trans. Systems, Man, Cybernetics* 1: 251–260, 1971.
34. SZENTÁGOTHAI, J. The elementary vestibuloocular reflex arc. *J. Neurophyiol.* 13: 395–407, 1950.

35. WARWICK, R. Representation of the extraocular muscles in the oculomotor nuclei of the monkey. *J. Comp. Neurol.* 98: 449–504, 1953.
36. YOUNG, L. R. The current status of vestibular system models. *Automatica* 5: 369–383, 1969.
37. YOUNG, L. R. AND STARK, L. Variable feedback experiments testing a sampled data model for eye tracking movements. *IEEE Trans. Profess. Tech. Group on Human Factors in Electron.* 4: 38–51, 1963.